

Evaluation of the 1s and 2s Subshell Properties of Fluorine and Neon Atoms and Their positive Ions Using the Hartree-Fock Approximation

Ahmed Jammel Mahdi¹ and Qassim Shamkhi AL-Khafaji²

^{1,2}Department of Physics, College of Science, Kufa University, Iraq

*Corresponding Author E-mail: ah.1998ir@gmail.com ²qasimsh.alkhafaji@uokufa.edu.iq

ARTICLE INF.

Article history:

Received: 6 JUN., 2025

Revised: 28 JUN., 2025

Accepted: 3 JUL., 2025

Available Online: 30 JUL., 2025

Keywords:

Hartree-Fock approximation, fluorine and neon ions, radial density function, inter-electronic distribution, ionization effects.

ABSTRACT

This is a comparative Hartree-Fock study of the atomic model systems for fluorine (F) and neon (Ne), along with their respective singly charged ions (F⁺ and Ne⁺), considering the ground-state configurations of the 1s and 2s subshells. In particular, this study evaluates one- and two-particle radial density distributions, inter-electronic distribution functions, and expectation values of both radial and inter-electronic distances, along with their standard deviations. This study also examines electron repulsion -the kinetic energy, electron-nucleus attraction energy, electron energy, and total Hartree-Fock energy. The results reveal significant spatial contractions and energetic stabilizations in the 2s subshell following ionization, but not in the 1s subshell. The results obtained in this study show the differential sensitivity to ionization of core and valence shells in a medium-light atomic system and are consistent with previously reported results. All calculations were conducted using a self-consistent field implementation of the Hartree-Fock method in Mathcad 15, with Slater-type orbitals expressed in atomic units.

DOI: <https://doi.org/10.31257/2018/JKP/2025/v17.i01.19788>

تقييم خصائص الغلاف الثانوي لذرتي الفلور والنيون وايوناتها الموجبة باستخدام طريقة هارترتي فوك

احمد جميل مهدي¹ و.د. قاسم شمخي الخفاجي²

قسم الفيزياء، كلية العلوم، جامعة الكوفة، العراق

الكلمات المفتاحية:

تقريب هارترتي-فوك
أيونات الفلور والنيون
دالة الكثافة الشعاعية
التوزيع بين الإلكترونات
طاقات الغلاف الفرعي 1 و2s
تأثيرات التآين.

الخلاصة

هذه دراسة مقارنة باستخدام هارترتي-فوك لأنظمة النماذج الذرية للفلورين (F) والنيون (Ne) وكذلك الأيونات أحادية الشحنة (F⁺) و (Ne⁺ على التوالي)، وتنتظر في تكوينات مواقف الحالة الأرضية للطبقتين الفرعيتين 1s و 2s. على وجه الخصوص، تقييم هذه الدراسة توزيعات الكثافة الشعاعية لجسيم واحد وجسيمين، ووظائف التوزيع بين الإلكترونات، والقيم المتوقعة للمسافات الشعاعية وبين الإلكترونات، إلى جانب انحرافات المعيارية. ستفحص هذه الدراسة أيضاً الطاقة الحركية، وطاقة جذب الإلكترونات إلى النواة، وطاقة تتافر الإلكترونات إلى الإلكترونات، والطاقة الكلية لهارترتي-فوك. تكشف النتائج عن انكماش مكاني كبير واستقرار في الطاقة في الطبقة الفرعية 2s بعد التآين، ولكن ليس في الطبقة الثانوية. تُظهر النتائج المعروضة هنا الحساسية التفاضلية لتآين

أغلفة النواة والتكافؤ في نظام ذري متوسط الضوء وهي متوافقة مع النتائج التي تم الإبلاغ عنها سابقًا. أجريت جميع الحسابات باستخدام تطبيق ميداني متسق ذاتيًا لطريقة هارترزي-فوك في برنامج ماثكاد 15، مع التعبير عن مدارات سلاتر بوحدات ذرية.

1. INTRODUCTION

The precise theoretical modeling of multi-electron atoms is still an important problem in quantum mechanics, due mainly to electron-electron interactions [1]. There are numerous theoretical approximations to solve this problem. Among these, the most widely used is the Hartree-Fock (HF) approximation. The HF approximation conceptualizes electrons moving independently in a mean field generated by all other electrons on average. From the HF approximation, a self-consistent description of the many-electron wave function of an atom is obtained [2].

In HF, the total wave function is a Slater determinant of the spin-orbitals. The Slater determinant guarantees that the total wave function is antisymmetric with respect to the exchange of any two electrons and also follows the Pauli exclusion principle. The spatial parts for the orbitals are typically Slater-type orbitals (STOs) to be constructed via an SCF process. HF is a reasonable option for the determination of ground state properties and investigation of atomic shell behaviour, although it does not account for dynamic correlation[3].

The HF formalism has been applied to dozens of atoms and ions of various atomic numbers and charge states [4]. Theoretical physical observables, such as radial electron distributions, various inter-particle distance functions, and components of energy (kinetic, attraction to nuclei, electron-electron repulsion), can be generated. There are reported studies that examined neutral

atoms and their singly ionized atoms, especially involving multiple second-period elements [5-7].

In this context, a Hartree-Fock analysis of fluorine (F) and neon (Ne) and their singly charged ions (F⁺ and Ne⁺) with careful attention paid to the 1s and 2s subshells. The changes in electronic structure due to ionization are analyzed by one- and two-particle radial density functions, $f(r_{12})$, and numerous expectation values, $\langle r_1^n \rangle$, $\langle r_{12}^n \rangle$ ($n = -2, -1, 0, 1, 2$), as well as their associated statistical measures such as standard deviations. We will also compute and analyze the kinetic energy, electron-nucleus attraction energy, electron-electron repulsion, and total Hartree-Fock energy for each subshell. This study aims to provide valuable information regarding the structural and electronic localization, and energetic behaviour during ionization of moderately light atoms. We examine the differences in behaviour between the inner-core (1s) and outer-valence (2s) electrons concerning their spatial distribution within the same shell structure. We contribute to a better understanding of shell-specific dynamics during atomic ionization, as illustrated by spatial distribution graphs, while establishing a foundation for subsequent computational and experimental work.

2 - Methodology

2-1 Hartree-Fock Approximation

The HF method describes the many-body wave function as a single

Slater determinant constructed from spin-orbitals [8]:

$$\begin{aligned} \psi_{n\ell m_s}(r, \omega) \\ = R_{n\ell}(r)Y_{\ell m}(\theta, \phi)\chi_s(\omega) \end{aligned} \quad 2.1$$

The spatial part of the atomic orbitals is defined using the standard normalized Slater-type orbital (STO), which generally has the following form:

$$\phi(r) = N \cdot r^{n-1}e^{-\zeta r}$$

where N is the normalization constant, ζ is the orbital exponent that characterizes the spatial extent of the orbital, and n is the principal quantum number (e.g., n = 1 for 1s and n = 2 for 2s orbitals). Slater-type orbitals are commonly used in atomic structure calculations because they provide reasonable electron localization very close to the nucleus and exhibit the correct asymptotic behavior at large distances.

Instead of performing the self-consistent field (SCF) calculation in an iterative fashion, the parameters n, N, and ζ were obtained from Roothaan's standard Hartree-Fock tables [9], which provide well-optimized basis functions for ground-state atoms. The advantage of using the Roothaan

tables is that the coefficients represent the basis sets with high accuracy, and no iterative optimization of the orbitals is required. The wavefunctions used in the radial and inter-electronic properties are consistent with quantum chemical benchmarks; therefore, while a full SCF loop was not performed, the underlying Hartree-Fock formalism remains valid.

The Roothaan coefficients provide a credible basis for further computation

of physical quantities such as electron density distributions and energy expectation values. In all cases, the functions were computed in atomic units (a.u.), and integrations were performed in Mathcad 15 using stringent numerical settings to ensure numerical stability and consistency throughout the calculations.

2-2 Slater Determinant

To satisfy the Pauli exclusion principle, the many-electron wave function is expressed as a Slater determinant, which is an antisymmetrized combination of single-electron spin-orbitals [10]:

$$\begin{aligned} \Psi_{HF}(r_1, r_2, \dots, r_N) \\ = \frac{1}{\sqrt{N!}} \begin{vmatrix} \psi_1(r_1) & \psi_2(r_1) & \dots & \psi_N(r_1) \\ \psi_1(r_2) & \psi_2(r_2) & \dots & \psi_N(r_2) \\ \vdots & \vdots & \ddots & \vdots \\ \psi_1(r_N) & \psi_2(r_N) & \dots & \psi_N(r_N) \end{vmatrix} \end{aligned} \quad 2.2$$

The antisymmetrized form guarantees that interchanging two electrons will only change the sign of the wave function. Each spin-orbital $\psi_i(r)$ consists of a spatial part and a spin part. The determinant structure inherently enforces the requirement that no two electrons occupy the same quantum state.

2-3 One-Particle Radial Density Function [11]

$$D(r_1) = \int |\psi(r_1, \theta, \phi)|^2 r_1^2 d\Omega \quad (2.3)$$

This function describes the probability of finding an electron at a distance r1 from the nucleus.

2-4 Two-Particle Radial Density Function [12]

$$D(r_1, r_2) = \iint \Gamma(r_1, r_2) r_1^2 r_2^2 d\Omega_1 d\Omega_2 \quad (2.4)$$

Describes the probability of finding two electrons at distances r_1 and r_2 .

2-5 Inter-Electron Distribution

Function [13]

$$f(r_{12}) = \iint |\Psi(r_1, r_2)|^2 \delta(|r_1 - r_2| - r_{12}) dr_1 dr_2 \quad (2.5)$$

This function describes the probability of a pair of electrons being separated at a distance r_{12} .

2-6 Expectation Values [14]

$$\langle r_1^n \rangle = \int_0^\infty r_1^n D(r_1) dr_1, \quad (2.6)$$

$$\langle r_{12}^n \rangle = \int_0^\infty r_{12}^n f(r_{12}) dr_{12}$$

To examine electron spatial behavior, calculations of expectation values $\langle r_1^n \rangle$ and $\langle r_{12}^n \rangle$ were performed for $n = -2, -1, 0, 1$, and 2 . Negative n values ($n < 0$) are close to the nucleus or minimal electron-electron distances, positive n values ($n > 0$) are the outer regions of electron distribution and wider spread.

2-7 Standard Deviations [15]

$$\Delta r_1 = \sqrt{\langle r_1^2 \rangle - \langle r_1 \rangle^2},$$

$$\Delta r_{12} = \sqrt{\langle r_{12}^2 \rangle - \langle r_{12} \rangle^2} \quad (2.7)$$

The standard deviations Δr_1 and Δr_{12} serve as quantitative indicators for both spatial dispersion and positional uncertainty among electrons.

2-8 Energy Components [16]

2-8-1 Kinetic Energy:

$$\langle T \rangle = -\frac{1}{2} \sum_i \langle \psi_i | \nabla^2 | \psi_i \rangle \quad (2.8)$$

2-8-2 Electron-Nucleus Attraction:

$$\langle V_{en} \rangle = - \sum_i \left\langle \psi_i \left| \frac{Z}{r} \right| \psi_i \right\rangle \quad (2.9)$$

2-8-3 Electron-Electron Repulsion:

$$\langle V_{ee} \rangle = \frac{1}{2} \sum_{i \neq j} \iint \frac{|\psi_i(r_1)|^2 |\psi_j(r_2)|^2}{|r_1 - r_2|} dr_1 dr_2 \quad (2.10)$$

2-8-4 Total Energy:

$$\langle E \rangle = \langle T \rangle + \langle V_{en} \rangle + \langle V_{ee} \rangle \quad (2.11)$$

The study involved assessing these energy components for the 1s and 2s subshells in both fluorine and neon atoms alongside their singly ionized cations to investigate ionization effects on inner and outer shell contributions.

3. Results and Discussion

All equations used in this study were processed in Mathcad 15, leveraging its symbolic and numerical integration capabilities. The calculations were performed in atomic units (a.u.) for consistency, with radial functions evaluated over the range of $r = 0.0001$ to 16 a.u. Numerical integrals (such as normalization and energy calculations) were performed using Mathcad's built-in integration engine, which offers high-precision symbolic and numeric integration tools. Roothaan's parameters for Slater-type orbitals were used as inputs to construct the atomic wavefunctions, enabling the accurate evaluation of expectation

values, energy components, and various distribution functions used in this study. The numerical results for the

neutral atoms and their singly-charged ions are listed in the following tables and figures.

Table 1 Peak Values and Radial Positions of the One-Particle Density Function $D(r_1)$ for the 1s and 2s Subshells of Fluorine and Neon Atoms and Their Ions.

Ion	Results and comparison	1s shell		2s shell			
		r_1	Dmax(r_1)	First peak		Second peak	
				r_1	Dmax(r_1)	r_1	Dmax(r_1)
F	P.w	0.11	4.6056	0.09	0.1978	0.77	1.055
	Ref.[17]	0.11	4.608	---	---	---	--
F ⁺	P.w	0.1151	4.615	0.0908	0.2123	0.7559	1.1109
Ne	P.w	0.1	5.1413	0.08	0.22671	0.68	1.1846
	Ref.[17]	0.10	5.137	---	---	---	---
Ne ⁺	P.w	0.1032	5.1468	0.0812	0.24117	0.6773	1.2393
	Ref.[7]	---	---	0.087	0.2395	0.674	1.2393

Table 2. Expectation Values and Standard Deviations of $\langle r_1^n \rangle$ for the 1s and 2s Subshells of Fluorine and Neon Atoms and Their Ions

Ion	shell	$\langle r_1^{-2} \rangle$	$\langle r_1^{-1} \rangle$	$\langle r_1^0 \rangle$	$\langle r_1^1 \rangle$	$\langle r_1^2 \rangle$	Δr_1
F	1s	150.85 095	8.630 4	1	0.17575	0.04 161	0.10 356
	Ref.[14]	150.83 417	8.630 362	---	0.175747	0.04 1612	---
	2s	8.6985	1.449	1	1.00102	1.21	0.46
F ⁺	1s	150.90	8.632	1	0.17567	0.04	0.1
	2s	9.2958	1.503	1	0.96088	1.10	0.09
	Ref.[7]	9.2958	1.503	0.9	0.960880	1.10	---
Ne	1s	187.20	9.618	1	0.15763	0.03	0.09
	Ref.[14]	187.19	9.618	---	0.157631	0.03	---
	2s	11.0711	1.632	1	0.89213	0.96	0.41
Ne ⁺	1s	187.27	9.620	1	0.15757	0.03	0.09
	2s	11.7351	1.685	1	0.86033	0.89	0.38

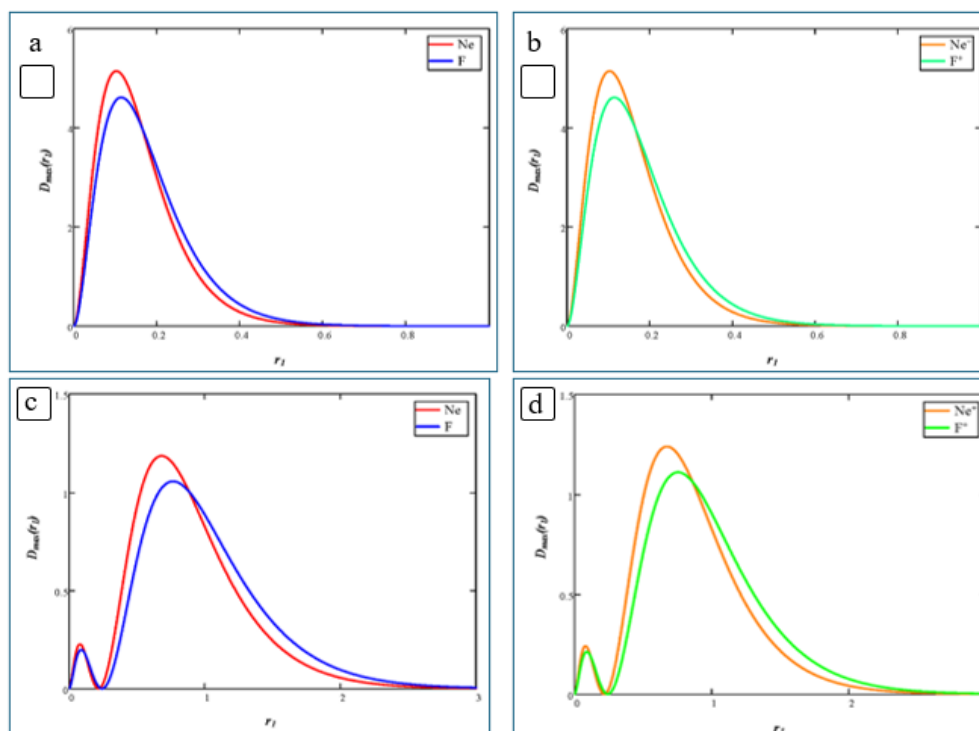


Figure 1. One-Particle Radial Density Distributions $D(r_1)$ for the 1s and 2s Subshells of Fluorine and Neon Atoms and Their Ions:

- (a) 1s subshell of F and Ne atoms,**
- (b) 1s subshell of F^+ and Ne^+ ions,**
- (c) 2s subshell of F and Ne atoms,**
- (d) 2s subshell of F^+ and Ne^+ ions.**

The data presented in Table 1 and the graphical representations provided in Figure 1 remains relatively stable upon ionization for the 1s subshell. The radial position and peak value of $D(r_1)$ remain nearly identical for both neutral and ionized F and Ne. This suggests that the tightly bound inner-shell electrons are unaffected by the removal of an outer-shell electron. However, divergence across atomic number in the height and radial position of the density peak. As atomic number increases from $Z = 9$ (F) to $Z = 10$ (Ne), the electron density increases and the shell correspondingly contracts, this is observed in both the radial peak locations and the expectation values of

$\langle r_1^{-1} \rangle$ and $\langle r_1^{-2} \rangle$, illustrating the stronger nuclear attraction that draws inner electrons closer to the nucleus.

Compared to the 1s subshell, the 2s subshell was relatively more sensitive to ionization and atomic number. After ionization, the peaks of $D(r_1)$ not only increased in height but also shifted inward, indicating greater electron localization and spatial contraction. For example, in the fluorine atom, the 2s peak value was $D_{\max}(r_1) = 1.055$ in the neutral state, whereas the peak value for F^+ indicates an increased value of $D_{\max}(r_1) = 1.1109$. Furthermore, and even more pronounced, the 2s density peak for Ne exhibited the highest peak density value $D_{\max}(r_1) = 1.1846$ which

represents a further increase in peak density due to comparatively greater nuclear attraction experienced as atomic number increases. The trends indicated above provide support the combined effect of

atomic number and ionization on the magnitude of 2s contraction. An increase in atomic number raises the density peak by reducing radial distance, owing to reduced shielding and stronger nuclear attraction.

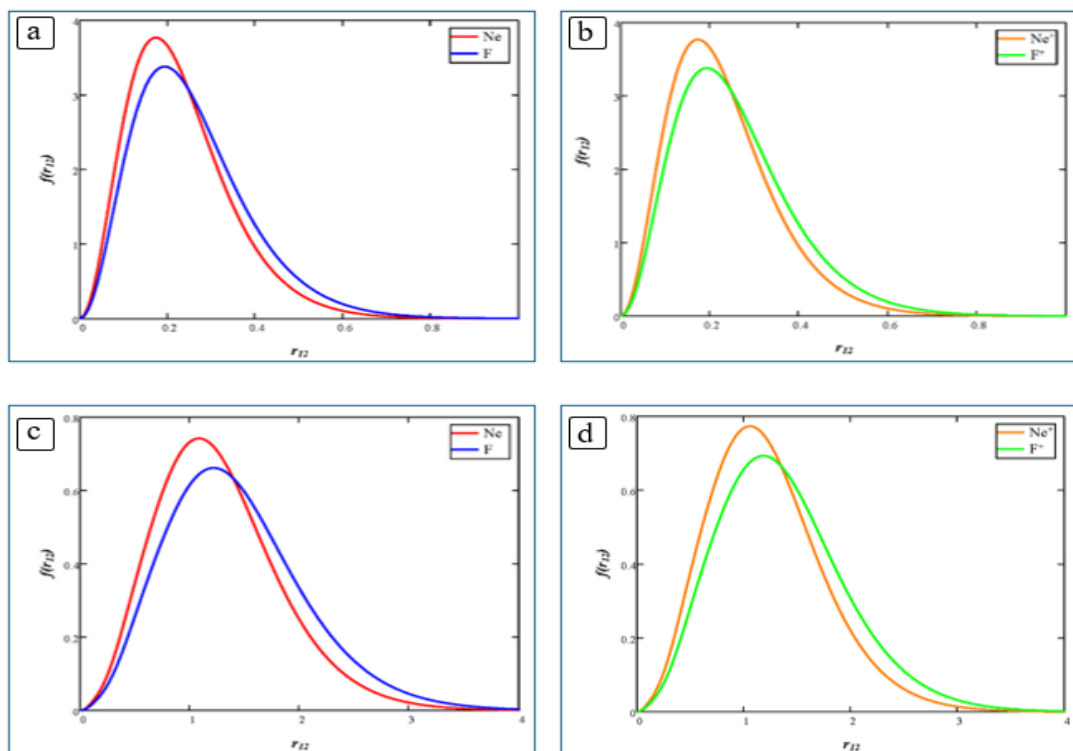
Ionization reduces the effect of electron-electron repulsion, further enhancing the contraction. Overall, while both representations demonstrate correlations between structural changes for the 1s and 2s subshells with ionization and atomic number, the changes observed for the 2s subshell are larger and more variable than those for the 1s subshell.

Table 3. Peak Values and Radial Positions of the Inter-Electronic Distribution Function $f(r_{12})$ for the 1s and 2s Subshells of Fluorine and Neon Atoms and Their Ions

Ion	s shell		2s shell	
	r12	$f_{max}(r_{12})$	r12	$f_{max}(r_{12})$
F	0.19	3.3798	1.22	0.66155
F ⁺	0.19	3.3815	1.19	0.69312
Ne	0.17	3.7688	1.08	0.7419
Ne ⁺	0.17	3.7705	1.06	0.77337

Table 4. Expectation Values and Standard Deviations of $\langle r_{12}^n \rangle$ for the 1s and 2s Subshells of Fluorine and Neon Atoms and Their Ions.

Ion	shell	$\langle r_{12}^{-2} \rangle$	$\langle r_{12}^{-1} \rangle$	$\langle r_{12}^0 \rangle$	$\langle r_{12}^1 \rangle$	$\langle r_{12}^2 \rangle$	Δr_{12}
F	1s	49.29297	5.35670	1	0.25683	0.08322	0.13137
	Ref.[17]	49.29188	5.35635	---	0.25692	0.08332	0.132
	2s	1.36426	0.91041	1	1.42309	2.43244	0.63816
F ⁺	1s	49.32167	5.35867	1	0.25672	0.08313	0.13123
	2s	1.46824	0.94569	1	1.36276	2.21674	0.59969
Ne	1s	61.24785	5.97179	1	0.23035	0.06694	0.11781
	2s	1.72157	1.02189	1	1.26870	1.93436	0.56987
Ne ⁺	1s	61.27510	5.97346	1	0.23024	0.06686	0.11770
	2s	1.83682	1.05682	1	1.22080	1.78110	0.53921



Inter-Electronic Distance Distributions $f(r_{12})$ for the 1s and 2s Subshells Figure 2. of Fluorine and Neon Atoms and Their Ions:

- (a) 1s subshell of F and Ne atoms,**
- (b) 1s subshell of F^+ and Ne^+ ions,**
- (c) 2s subshell of F and Ne atoms,**
- (d) 2s subshell of F^+ and Ne^+ ions.**

The inter-electronic distribution function $f(r_{12})$ describes the average inter-electronic distance within atomic shells. The findings in Tables 3 and 4, illustrated in Figure 2, suggest that the 1s shell is only marginally affected by ionization compared with the 2s shell, which is highly sensitive to ionization.

The position of the peak r_{12} and $f_{\max}(r_{12})$ for the 1s subshell remains largely unchanged after ionization, showing a negligible effect on the tightly bound core electrons (e.g., for $F \rightarrow F^+$, value of the r_{12} remains constant 0.19 a.u., while the value of $f_{\max}(r_{12})$ increases from 3.3798 to 3.3815).

In contrast, when comparing fluorine ($Z = 9$) with neon ($Z = 10$), the

1s shell exhibits a slight shift inward (from 0.19 to 0.17 a.u.) and a slight increase in peak height (from 3.76 to 3.77), owing to greater electron confinement and increased nuclear attraction.

The 2s shell clearly shows changes.

Ionization of neon leads to a decrease in the inter-electronic distance r_{12} from 1.08 a.u. (Ne) to 1.06 a.u. (Ne^+), demonstrating contraction of electrons locally within atomic subshells. Concurrently, an increase in peak value from 0.7419 to 0.7734 suggests a compression of the electron-electron repulsion distribution, indicating more closely held electrons.

The results in Table 4 reinforce this finding using expectation values of $\langle r_{12}^n \rangle$. For the 2s shell, the decrease in $\langle r_{12} \rangle$, $\langle r_{12}^2 \rangle$ and the standard deviation Δr_{12} are likely evidence of the effective tightening of electron distribution upon ionization. In larger-Z atoms, stronger electron interactions are evidenced by smaller $\langle r_{12} \rangle$ and larger $\langle r_{12}^{-1} \rangle$ values in neon Ne compared with Fluorine (F).

The plots of $f(r_{12})$ in Figure 2 clearly illustrate the following:

Panels (a) and (b) exhibit the degree of overlap of distributions for 1s electrons confirming the rigidity of the 1s shell.

Panels (c) and (d) demonstrate reduced inter-electronic spacing with

increasing atomic number. The effect of ionization is related to increasing correlation among electrons within the 2s shell, which persists in the corresponding ions.

In conclusion, the results from the inter-electronic distribution functions show the 1s shell remains predominantly unchanged, while the 2s shell contracts significantly with both ionization and increasing atomic number. The study suggests that, for ions, the effects of electron repulsion and localization become more pronounced with increasing atomic number, consistent with observations in other multi-electron Hartree-Fock studies.

Table 5 Values of energy components in the 1s and 2s subshells

Ion	shell	$\langle V_{ee} \rangle$	$-\langle V_{en} \rangle$	$-\langle V \rangle$	$\langle T \rangle$	$-\langle E_H \rangle$
F	1s	5.35670	155.34721	149.99052	74.99526	74.99526
	Ref.[17]	5.35635	155.32938	149.97303	74.98652	74.98652
	2s	0.91041	26.09509	25.18468	12.59234	12.59234
F⁺	1s	5.35867	155.38687	150.02820	75.0141	75.0141
	2s	0.94569	27.05967	26.11398	13.05699	13.05699
Ne	1s	5.97179	192.36149	186.38970	93.195	93.195
	2s	1.02189	32.65092	31.62903	15.81451	15.81451
Ne⁺	1s	5.97346	192.40079	186.42732	93.21366	93.21366
	2s	1.05682	33.71068	32.65385	16.32693	16.32693

The energetic behavior of the 1s and 2s subshells under ionization and increasing atomic number is shown in Table 5. This Table contains the expectation values for electron-electron repulsion energy $\langle V_{ee} \rangle$, electron–nucleus attraction energy $\langle V_{en} \rangle$, total potential energy $\langle V \rangle$, kinetic energy

$\langle T \rangle$, and total Hartree-Fock energy $\langle E_H \rangle$.

For the 1s subshells, all their energy components remain nearly unchanged upon ionization, demonstrating that the 1s subshell lies in the deepest potential well and is strongly shielded from changes in outer shells. For example, F has $\langle T \rangle = 74.99526$ and F⁺ has $\langle T \rangle = 75.0141$,

while both $\langle V_{en} \rangle$ and $\langle V_{ee} \rangle$ remain virtually unchanged. A similar trend is observed for neon (Ne); this provides quantitative evidence of the insensitivity of the 1s shell to the removal of outer electrons.

For the 2s subshell, significant energy changes occur following ionization of the outer electrons. All energy components increase upon ionization.

- In F, the kinetic energy $\langle T \rangle$ increases from 12.592 to 13.057 and $-\langle V \rangle$ increases from 25.18 to 26.11 a.u.
- In Ne, kinetic energy $\langle T \rangle$ increases from 15.81 to 16.32 a.u., reinforcing the idea that electron confinement increases as screening decreases.

With increasing nuclear charge from F to Ne, the electron-nucleus attraction intensifies, causing the total energies of both the 1s and 2s subshells to become more negative, despite minor increases in electron-electron repulsion. For example, the total Hartree-Fock energy $-\langle E_{HF} \rangle$ for the system decreases significantly from -12.59 a.u. (F) to -15.81 a.u. (Ne), indicating greater stabilization, confinement, and electronic localization.

In general, energetic stabilization in the 2s shell is accompanied by increased kinetic energy upon ionization, whereas the 1s shell is largely unaffected. Furthermore, increases in atomic number have a significant impact on the potential well for both subshells. This is reinforced by the increasing influence of nuclear attraction on the electronic structure.

These results are consistent with previous Hartree-Fock studies based on the self-consistent field (SCF) method.

4 - Conclusions

The research presented here has analyzed the 1s and 2s subshells of fluorine (F) and neon (Ne) and singly ionizing ions (F^+ , Ne^+) using the time-independent Hartree-Fock approximation (HF). The important findings of the research are:

1. The radial and inter-electronic distributions for the 1s shell were nearly indistinguishable across the entire group of studied systems, showing only slight changes as a function of ionization and atomic number variations.

2. Ionization caused contraction of the 2s, inferred by sharper $D(r_1)$ and $f(r_{12})$ peaks, smaller $\langle r_1 \rangle$ and $\langle r_{12} \rangle$, and reductions in radial spread.

3. In the absence of ionization, increasing nuclear charge compressed the electron cloud from F to Ne, resulting in a compression of both the 1s and 2s shells, which reflects stronger nuclear binding.

4. The ionized cases showed a significantly contracted ionic 2s shell, especially in Ne^+ , as seen by the sharper peak in $f(r_{12})$, which reflects stronger spatial localization of electron pairs.

5. Ionization increased the absolute magnitudes of $\langle T \rangle$, $\langle V_{en} \rangle$, $\langle V_{ee} \rangle$, and $\langle E \rangle$ for the 2s shell; conversely, the energies for the 1s shell remained largely intact, showing the independence of the response to ionization changes.

6. The ionization primarily affected the behavior of the 2s (valence) charge; there is no observable structural or energetic change the 1s (core) electron density in this study.

7. the HF method has demonstrated it can capture subshell-specific effects resulting from nuclear charge and ionization in light atoms.

5 - Reference

- [1] F.-s. Liu, *Advanced quantum mechanics upon theorems (Physics research and technology)*. Hauppauge, New York: Nova Science Publisher's, Inc., 2014, pp. x, 268 pages.
- [2] T. Veszprémi and M. Fehér, *Quantum Chemistry: Fundamentals to Applications*. Springer US, 2012.
- [3] P. d'Avenia, L. Maia, and G. Siciliano, "Hartree-Fock type systems: Existence of ground states and asymptotic behavior," *Journal of Differential Equations*, vol. 335, pp. 580-614, 2022/10/25/ 2022.
- [4] M. A. Jones, H. J. Vallury, C. D. Hill, and L. C. L. Hollenberg, "Chemistry beyond the Hartree-Fock energy via quantum computed moments," *Sci Rep*, vol. 12, no. 1, p. 8985, May 28 2022.
- [5] K. H. AL-Bayati, W. A. Hussein, and M. A. H. Mahmood, "Calculation of Radial Density Distribution Function for main orbital of Carbon atom and Carbon like ions," *Baghdad Science Journal*, vol. 11, no. 4, pp. 1455-1458, 2014.
- [6] K. Banyard and J. Moore, "Angular and radial correlation effects in momentum space for H-, He and Li+," *Journal of Physics B: Atomic and Molecular Physics*, vol. 10, no. 14, p. 2781, 1977.
- [7] M. Al-Sharaa, Q. S. AL-Khafaji, S. Kadhim, and M. Al-Quraishi, "Calculation the Radial Electronic Density Distribution and the One Electron Expectation Value for(2s2) Configuration for $4 \leq Z \leq 15$," *Library Progress (International)*, pp. 189-196, 09/19 2024.
- [8] P.-O. Löwdin, "Quantum theory of many-particle systems. II. Study of the ordinary Hartree-Fock approximation," *Physical Review*, vol. 97, no. 6, p. 1490, 1955.
- [9] E. Clementi and C. Roetti, "Roothaan-Hartree-Fock atomic wavefunctions: Basis functions and their coefficients for ground and certain excited states of neutral and ionized atoms, $Z \leq 54$," *Atomic data and nuclear data tables*, vol. 14, no. 3-4, pp. 177-478, 1974.
- [10] C. C. Lu, *Relativistic Hartree-Fock-Slater eigenvalues : radial values, and potentials for atoms*. New York: Academic Press (in English), 1971.
- [11] H. A. Abd Alabas, Q. S. AL-Khafaji, and A. H. Raheem, "A Theoretical Study of the Atomic Properties for Subshells of N and O Using Hartree-Fock Approximation," *International Journal of Physics*, vol. 4, no. 4, pp. 74-77, 2016.
- [12] R. Dosh, "Study Of Atomic Properties Of Three Electron Systems

Using Hartree-Fock Approximation," College of Sciences Department of Physics, University of Kufa, 2012. [Online]. Available:

[13] V.-M. Ene, I. Lianu, and I. Grosu, "Hartree-Fock approximation for non-Coulomb interactions in three and two-dimensional systems," *Physics Letters A*, vol. 529, p. 130064, 2025/01/05/ 2025.

[14] S. L. Saito, "Hartree-Fock-Roothaan energies and expectation values for the neutral atoms He to Uuo: The B-spline expansion method," *Atomic Data and Nuclear Data Tables*, vol. 95, no. 6, pp. 836-870, 2009/11/01/ 2009.

[15] S. Kadhim, "Study the atomic properties of 2s shell for some atoms," *Iraqi Journal of Physics (IJP)*, vol. 11, pp. 20-26, 01/01 2013.

[16] M. H. AL-Quraishi and Q. S. AL-Khafaji, "Evaluation of the Hartree-Fock Energy of Four Electron Systems," *NeuroQuantology*, vol. 20, no. 6, pp. 4115-4121, 2022.

[17] Q. Shamkhi, "Calculation of The Energies of k-shell for Atoms ($Z=8$ to 10) by using Hartree-Fock Method," *Journal of Kufa-physics*, vol. 6, no. 1, 2014.